Review Article

Recent Advances in Dynamic Monitoring of Drug Release of Nanoparticle Using Förster Resonance Energy Transfer and Fluorescence Lifetime Imaging

Shih-Hsun Cheng,[a,b,†] Nai-Tzu Chen,[a,c,†] Chia-Yan Wu,[a] Chao-Yu Chung,[d] Yeukuang Hwu,[d,e] Chung-Yuan Mou,[c] Chung-Shi Yang[f] and Leu-Wei Lo[a,*]

[a]*Division of Medical Engineering Research and* [f]*Center for Nanomedicine Research, National Health Research Institutes, Zhunan, Taiwan, R.O.C.*

[b]*Institute of NanoEngineering and MicroSystems, National Tsing Hua University, Hsinchu, Taiwan, R.O.C.*

[c]*Department of Chemistry, National Taiwan University, Taipei, Taiwan, R.O.C.*

[d]*National Synchrotron Radiation Research Center, Hsinchu, Taiwan, R.O.C.*

[e]*Institute of Physics, Academia Sinica, Taipei, Taiwan, R.O.C.*

Received June 12, 2011; Accepted August 9, 2011; Published Online August 25, 2011

In this review, we summarized the recent advances in dynamic monitoring of drug release of nanoparticle using FRET and FLIM. Using FRET to understanding the dynamics of drug released from its nanocarrier within intracellular milieu provides high sensitivity and temporal information of the releasing profile. Such information is crucial for the design of drug carriers and validation of drug controlled release. This approach thus has been prevailingly used in monitoring of drug release from a variety of DDS, including quantum dot-, polymer-, and silica-based delivery systems. Alternatively, FLIM assessing changes of micro-environment of drug possesses great potential for use in profiling the intracellular drug release and subcellular drug distribution with various DDS. Our recent approach using FLIM for mapping the intracellular Dox released from pH-responsive MSN has exemplified the feasibility of delineating subcellular distribution of fluorescent drug with corresponding variation of fluorescence lifetime. Both FRET and FLIM are emerging as important techniques in assessing the efficiency of targeted delivery and controlled release of drug with different nanodelivery systems.

Keywords: FRET; FLIM; Drug release dynamics; Nanoparticle.

INTRODUCTION

Nanotechnology has shown tremendous promise in drug delivery systems (DDSs) for increasing the efficacy of pharmaceuticals since improved pharmacokinetics and biodistribution.[1] A wide variety of nanomaterials such as liposomes, micelles, and inorganic nanoparticles have been employed as drug deliveries.[2,3] Although passive and targeted drug delivery systems have addressed lots of important issues, additional properties that can be included in nanocarrier systems to enhance the bioavailability of drugs at the therapeutic site and cellular internalization, are very important.[4,5] Nano DDS incorporated with stimuli-responsive property (e.g., light, pH, temperature, or redox potential), for instance, would be amenable to address some of the systemic and intracellular delivery barriers.[6] There are many reviews to discuss the stimuli-responsive nanocarrier systems for drug delivery.[6] The advancement in material science has led to design of a variety of materials, which are used for development of nanocarrier systems that can respond to biological stimuli.[6-14] With greater understanding of the difference between normal and pathological tissues and cells and parallel developments in material design, there is a highly promising role of stimuli-responsive nanocarriers for drug delivery in the future. Thus, being able to monitor the dynamic release of drugs delivered from the nanocarriers following stimuli in the biological system is

Special issue for the nanotechnology-related analytical chemistry

* Corresponding author. Tel: +886-37-246166 ext. 37115; Fax: +886-37-586440; E-mail: lwlo@nhri.org.tw

† These authors contributed equally to this work

becoming critical in validation of the design of DDS in its biomedical applications.

In review of the advances of functionalized nanomaterials used for DDS in recent years, a number of so-called theranostic nanoparticles which composed of dual diagnostic and therapeutic utilities have been built up with functionalities of contrast signal, therapeutic payload, drug carrier, and targeting ligand.[15-22] The contrast signals containing certain unique optical, magnetic, or radioactive property can emit physical signals spontaneously or upon excitation by an external source. The physical or chemical interaction between signal source and therapeutic payload induced from biological environment could be used to monitor the dynamics of therapeutic drug release. In order to generate the stimulation-responsive release of drug, scientists design a variety of "switch" linkages which can be activated by external stimuli such as light (trans-cis molecules),[23] pH value (hydrazone),[24] redox (disulfide bonding)[25] or enzyme responsive system.[26] In this review we attempt to summarize the current advances in monitoring of drug release of nanocarriers using Förster resonance energy transfer (FRET) analysis and fluorescence lifetime imaging microscopy (FLIM).

The fluorescence-based imaging modality with the aid of FRET or fluorescence quenching is an efficient tool for tracking dynamics of therapeutic drug release. In the case of using FRET technique to monitor drug release, two types of fluorophores are incorporated into the core of drug-carrying nanoparticles for use as energy donor and acceptor respectively. Since FRET interactions are donor-acceptor distance-dependent, FRET occurs only in intact nanoparticle which carriers with intimate contact of donor-acceptor pairs. Once the nanoparticle carriers become disintegrated upon external stimuli, these fluorophores are discharged from the carrier and diffuse outwards. It consequently increases the average distance between the donors and acceptors, resulting in a decrease of FRET signal. Such a variation of FRET in intensity or lifetime can be captured and analyzed by fluorescence imaging microscopy to visualize dynamics of drug release from nanocarriers. Additionally, the occurrence of FRET causes the fluorescence lifetime of donor to decrease, which can be detected using FLIM. FLIM is an imaging technique for producing an image based on the differences in the exponential decay rate of the fluorescence from a fluorescent sample.[27-30] Efficient FRET can be quantitatively analyzed by lifetime imaging maps of FLIM system. The energy transfer efficient rate (K_{ET}) is calculated from $K_{ET} = 1 - \tau_2/\tau_1$, of which fluorescence lifetime is corresponding to the presence (τ_2) or absence (τ_1) of FRET28. This approach allows quantitative mapping of the relative concentration between nanocarrier-bound and -unbound therapeutic drugs in cells.

Quantum Dot-Based Drug Delivery System and Sensors

Quantum dot (QD) serves as a great candidate for nanodelivery and tracer in biological application. Owing to its advantages in photostability and resistance of photobleaching as compared to conventional organic fluorophores, a number of reports used QD as the drug carrier and monitored the dynamics of drug release of QD using FRET.[31,32] QDs have been wildly exploited as efficient FRET donors due to their photoluminescence characterized with broad absorption and narrow emission (few spectral cross-talk) that makes the selection of acceptor easy[31,32]

Leong's group developed a single-step quantum dot-mediated system (QD-FRET) to investigate the structural composition and dynamic behavior of plasmid DNA nanocomplex in the cell.[33] The QD-FRET system was using 605 nm QD as the donor conjugated onto the plasmid DNA (pDNA), whereas Cy5 was used as the energy transfer acceptor. The result is an ultrasensitive system to detect the dynamic release of DNA vectors from the nanocomplex. The FRET signal is abrogated as pDNA releases into the cytosol. Since the protection of pDNA from potential enzymatic barriers such as nuclease-mediated DNA degradation depends greatly on the stability of nanocarriers, by using QD-FRET system, the authors were able to develop an integrated sensing platform whereby both pDNA release and subsequent degradation can be simultaneously monitored. Furthermore, the same group demonstrated a two-step FRET system: the two-step energy transfer is constructed from the QD donor to the first acceptor of a nuclear dye (ND) (1st energy transfer, E12), and ND serve as a relay donor to the second acceptor Cy5 (2nd energy transfer, E23).[34,35] With this two-step QD-FRET system, the strategies of QD labeled pDNA of gene carrier were monitor by combinations of FRET-mediated emission from the ND and Cy5. For stable compact nanocomplexes, the QD donor drives energy transfers through the ND which acts as a relay to Cy5 conjugated on the polymeric gene carrier (E12 and E23 are "on"). While the nanocomplex begins to unpack and release intact pDNA, the E23 is off (Emission of Cy5 is diminished) and only the ND is 'on'. Finally, the

E12 is "off" due to the degradation of free pDNA. This approach can monitor both polyplex dissociation and pDNA degradation simultaneously within cells. Chen's group developed a new quantum dot (QD)-aptamer (apt) beacon that acts by folding-induced dissociation of a DNA intercalating dye, BOBO-3(B), is demonstrated with label-free thrombin detection.[36] The beacon is constructed by (1) coupling of a single-stranded thrombin aptamer to Qdot 565 via EDC/Sulfo-NHS chemistry and (2) staining the duplex regions of the aptamer on QD with excess BOBO-3 before thrombin binding. When mixing a thrombin sample with the QD-apt beacon, BOBO-3 is competed away from the beacon due to target-induced aptamer folding, which then causes a decrease in QD FRET-mediated BOBO-3 emission and achieves thrombin quantitation.

In another approach, QDs were introduced as a traceable marker and a carrier for delivery of siRNA.[37-39] Lee et al. reported a siRNA/QD-PEI complexe for analysis of intracellular siRNA uptake as well as the quantitative evaluation of siRNA unpacking from the cationic QD carriers by FRET analysis.[40] The authors used flow cytometric analysis to study the FRET interactions between cyanine dye labeled siRNA (cy5-siRNA) and cationic QD carriers. In addition, QD-PEI was further modified with a protein transduction domain (PTD) from protein transduction domain peptide (Hph-1). The siRNA/QD-PEI complexes with and without Hph-1 have displayed different unpacking kinetics of cy5-siRNA and intracellular uptake behaviors. This study demonstrated that siRNA/QD-PEI complexes can be utilized for intracellular trafficking of siRNA release, to maximize the silence of targets.

Bagalkot et al. developed the new design of QD-based theranostics for simultaneous imaging and therapeutic uses.[41] The multifunctional QD-aptamer (QD-Apt) was conjugated with the targeting modality of RNA aptamer to pinpoint the prostate-specific membrane antigen (PSMA) expressed in LNCaP cells. Instead of targeting, the double-stranded RNA aptamer was additionally used to intercalate anticancer drugs doxorubicin (Dox) for therapeutic modality. In this bi-FRET (dual donor-quencher) system, the QD fluorescence was quenched by Dox and the fluorescence of Dox was quenched by the RNA aptamers. While the Dox was loading, both QD and Dox fluorescence were turned "OFF" through bi-FRET. When the QD-Apt complex was treated with prostate cancer cells and Dox was gradually released, both QD and Dox fluorescence switched to "ON". This multifunctional QD-Apt-Dox delivered Dox to PSMA-expressing LNCaP cells more efficiently compared to non-targeted PC3 cells, and the efficacy of Dox delivery was monitored by FRET spontaneously.

QD-incorporating liposomes have been widely used as nonviral drug carriers, in which QDs are typically incorporated into the lipid bilayer of liposome to functionalize as fluorescence trackers.[42-44] The QD-liposome (QD-L) system was developed as a theranostic DDS for encapsulating Dox or other water-soluble drug molecules.[42-44] Weng et al. have developed the covalently conjugated hydrophilic, polymer-functionalized QD into outer layer of liposomes with the polyethylene glycol chains coating and then loaded Dox into the core of vesicles.[45] Tian et al developed the drug-loaded QD-L-Dox hybrid vesicles for theranostic modalities.[46] Gopalakrishnan et al. have also developed the hybrid QD-L system and used the fluorescence correlation spectroscopy (FCS) measurements to monitor the diffusion of QD while the liposome was fusing into cell plasma membrane.[42] The QDs in the plasma membrane and in the lipid bilayer were nearly identical but the solution of QD in small unilamellar vesicles was shown much slower diffusion.

Suzuki et al. explored a variety of FRET-based QD biosensors.[47] Fluorescent acceptors were immobilized on QDs, which serve in turn as their FRET donors. They demonstrated FRET-based QD bioprobes individually able to detect the actions of protease, deoxyribonuclease, DNA polymerase, and pH change. In addition, this was the first report of dual monitoring in such QD systems for multiplex detection of the action of a protease of trypsin in the presence of deoxyribonuclease.

Polymer-Based Drug Delivery System

Chen et al. developed the polymer micelle for drug delivery and revealed the release of hydrophobic molecules by FRET.[48] The dual labeled polymeric micelles containing fluorescently labeled copolymers and hydrophobic fluorescent probes entrapped in the polymeric micelle core. It is generally assumed that cellular uptake of hydrophobic probes was much faster than that of labeled copolymers. The hydrophobic probes in the core released from micelles in the extracellular space were observed in real-time using FRET imaging and spectroscopy. Both lipophilic tracers of DiI and DiO dyes were loaded into monomethoxy poly-(ethylene glycol)-block-poly(D,L-lactic acid) micelles as FRET pair. By monitoring the FRET efficiency, the results show that micelles exhibit membrane-mediated transporta-

tion of hydrophobic molecules into cells. In addition, the decrease of FRET on the plasma membrane was also observed in the treatment of paclitaxel-loaded micelles. By the results, they proposed that the fast release was facilitated by the poly(ethylene glycol) (PEG) shell in micelles. The transfer of hydrophobic molecules from micelle core into lipid membrane could be bridged by the high-density PEG.

Sung's group synthesized the pH-responsive doxorubicin (DOX)-loaded NPs, made of N-palmitoyl chitosan bearing a Cy5 moiety (Cy5-NPCS).[49] While the NPCS were internalized into cells, the intracellular pH value caused the DOX release. The caveolae-mediated endocytosis is the major pathway in the internalization of NPCS NPs. By using FRET, they observed that the DOX fluorescence was first seen in the cytosol while the NPs were stayed in the slightly acidic early endosomes. Then, more release of DOX was observed while NPs in late endosomes/lysosomes. Finally, the released DOX was subsequently accumulated in the nuclei and caused significant cytotoxicity. Understanding the fate of NPs with respect to their intracellular localization and drug release behavior is crucial for the rational design of drug carriers.

Chen's group fabricated the multifunctional magnetic nanocarrier for synchronous cancer therapy and sensing.[50] The nanocarrier was synthesized by coupling doxorubicin (DOX) to adipic dihydrazide-grafted gum arabic modified magnetic nanoparticles (ADH-GAMNP) via pH-sensitive hydrazone bond. ADH-GAMNP-DOX exhibited pH-triggered release of DOX in an acidic environment (pH 5.0). The fluorescence of DOX was self-quenched initially on GAMNP. By monitoring the change in the fluorescence intensity of DOX-ADH-GAMNP, the release of DOX can be sensed and functions as therapeutics subsequently.

Mesoporous Silica Nanoparticle-Based Drug Delivery System

In previous study, our group developed the intracellular pH-responsive mesoporous silica nanoparticles (MSN) for the controlled release of anticancer chemotherapeutics.[51] We synthesized the large pore MSN and incorporated the fluorescence dye Atto-647 in the framework. Additionally, the pH-sensitive linker was conjugated onto MSN nanochannel surfaces by hydrazone bonds. Then, another hydrazide group was further conjugated with doxorubicin. The pH-sensitive linkers, when loaded with drug, possessed two hydrazone bonds that were cleavable at endosomal pH. To verify the pH-sensitive release mechanism, we exploited fluorescence spectroscopy and imaging to demonstrate the release of doxorubicin from Atto-647-MSN-hydrazone-Dox. In this case, the Dox is the donor and Atto-647 of MSN is the acceptor. While the Dox encapsulated in Atto-647-MSN-hydrazone-Dox, two emission maximal peaks were observed using excitation of Dox at 440 nm: one at 580 nm from Dox and the other at 670 nm from Atto-647 via FRET from Dox. Following release of doxorubicin from nanoparticles at pH 4.5, the emission spectra of specimens excited at 440 nm indicated the decrease of fluorescence intensity of both doxorubicin and Atto-647. It was due to the decrease of doxorubicin concentration serving as FRET donor at pH 4.5. This result provides evidence for the pH-responsive release of doxorubicin.

Alternatively, fluorescence lifetime imaging microscopy (FLIM) can be exploited for dynamic monitoring of Dox release form the pH-responsive MSN. Optical imaging of specific molecular target and pathway in living cell has recently become possible through continuous development in high-resolution microscopy. FLIM, a noninvasive technique, can spatiotemporally monitor cellular events in physiological condition at single cell level and assess small changes in cellular environment around fluorescent chromophores. Therefore, FLIM could be a powerful tool to profile the drug release from nanoparticle. Most studies on the trace of nanoparticle were monitoring the bio-distribution in animal model and interaction between different moieties. In contrast, little information is available about the drug-release behavior which describes the dynamic profile of drug dissociation from its nanoparticle carrier intracellularly. Base on the environmental changes of drug during the release process from nanoparticle, fluorescence lifetime can be detected at last in one of these three scenarios: (1) the fluorescence lifetime of drug conjugated to nanoparticle; (2) the fluorescence lifetime of free drug which was released from nanoparticle; (3) the fluorescence lifetime of released drug which interacts or associates with cellular organelles. Hydrolysis of pH-sensitive linker's hydrazone bond in the acidic environment of endosomes/lysosomes releases doxorubicin (Dox) intracellularly from the MSN's nanochannels. While MSN-Dox is internalized by cell via endocytosis, cleavage of hydrazone bond takes place at local pH values in the range of 4 to 6 – corresponding to those found within endosomes and lysosomes. In our recent study,[52] approximately 24 hrs after the addition of ei-

ther free doxorubicin or MSN-Dox to plated cells,[53] the subcellular fluorescence lifetime distributions were assessed under FLIM. We excited samples with Dox treatments at 488 nm and measured both their Dox-corresponding fluorescence intensities and lifetimes at 520-570 nm. The fluorescence lifetime distribution from 0.5 to 4 ns presented by rainbow color from blue to red. Figure 1(a) shows the fluorescence lifetime distribution of free Dox in HeLa cell. An obviously different fluorescence lifetime distribution was detected within different cell compartments such as cytoplasm and nucleus. Fluorescence lifetime histograms whose maxima represent the average fluorescence lifetimes (τ_{av}) of Dox: 1.68 ns in the nucleus and 3.12 ns in the cytoplasm (Fig. 1(b)). It indicates that fluorescence lifetimes reflect the different subcellular micro-environments of Dox. The Dox intercalated with compact DNA in nucleus possesses much shorter fluorescence lifetime compared to that of Dox associated with intracellular components in cytoplasm. By contrast, in the case of MSN-Dox treated cell, the fluorescence lifetime distribution of Dox shows no significant difference between nucleus and cytoplasm. The average fluorescence lifetime is 1.80 ns in nucleus and 1.62 ns in cytoplasm (Fig. 1(c) and (d)). However, the latter should be the fluorescence lifetime of MSN-Dox invaginated within endosome/lysosome in cytoplasm. This indistinguishable lifetime distributions might result from that τ_{av} of Dox conjugated onto the nanochannels of MSN is incidentally similar to τ_{av} of Dox intercalated with DNA in nucleus. To further differentiate such close fluorescence lifetimes, using ultrafast laser for excitation to resolve the difference of fluorescence lifetime in picoseconds or shorter, or deceasing the Dox lifetime in MSN's nanochannels by incorporation of fluorescence quenchers in the MSN's framework to distinct the MSN-Dox lifetime from that in nucleus are two feasible approaches. With current measurements, although the lifetime of Dox in MSN (1.62 ns) is similar to Dox in the nucleus (1.80 ns), it is still significantly different from that of free Dox in cytoplasm (3.12 ns). Given that, we can use FLIM to profile the release of Dox from MSN after endocytosis by interpretation of the lifetime differences, corresponding to the changes of Dox situated in various subcellular micro-environments.

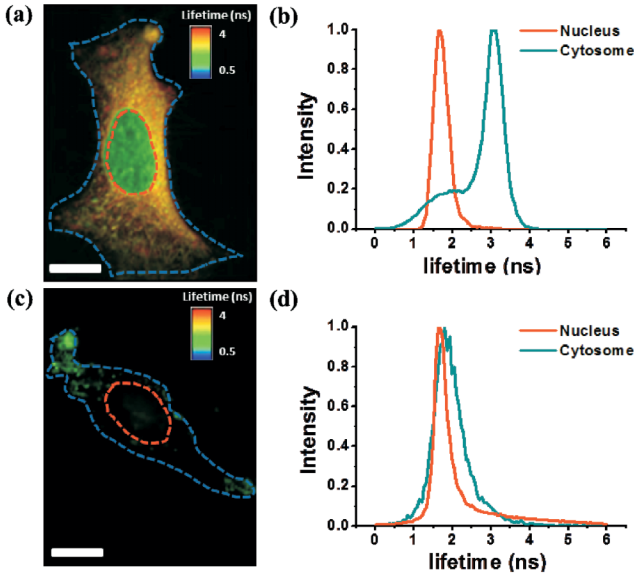

Fig. 1. Mapping of intracellular drug delivery and subcellular distribution using FLIM. (a) (b) Fluorescence lifetime imaging of Dox and its corresponding lifetime histogram as located in nucleus and cytoplasm after treating cells with free Dox for 24 hours. (c) (d) Fluorescence lifetime imaging of Dox and its corresponding lifetime histogram as located in nucleus and cytoplasm after treating cells with MSN-Dox for 24 hours. Blue and red dash lines delineate the cell membrane and nucleus envelope, respectively. The scale bar is 10 μm.

CONCLUSION

In this review, we summarized the recent advances in dynamic monitoring of drug release of nanoparticle using FRET and FLIM. Using FRET to understanding the dynamics of drug released from its nanocarrier within intracellular milieu provides high sensitivity and temporal information of the releasing profile. Such information is crucial for the design of drug carriers and validation of drug controlled release. This approach thus has been prevailingly used in monitoring of drug release from a variety of DDS, including quantum dot-, polymer-, and silica-based delivery systems (Scheme I). Alternatively, FLIM assessing changes of micro-environment of drug possesses great potential for use in profiling the intracellular drug release and subcellular drug distribution with various DDS. Our recent approach using FLIM for mapping the intracellular Dox released from pH-responsive MSN has exemplified the feasibility of delineating subcellular distribution of fluorescent drug with corresponding variation of fluorescence lifetime. Both FRET and FLIM are emerging as important techniques in assessing the efficiency of targeted delivery and controlled release of drug with different nanodelivery systems.

Scheme I FRET monitoring of drug release from a variety of DDS, including (A) quantum dot-, (B) quantum dot-lipid, (C) polymer-, and (D) mesoporous silica-based delivery systems

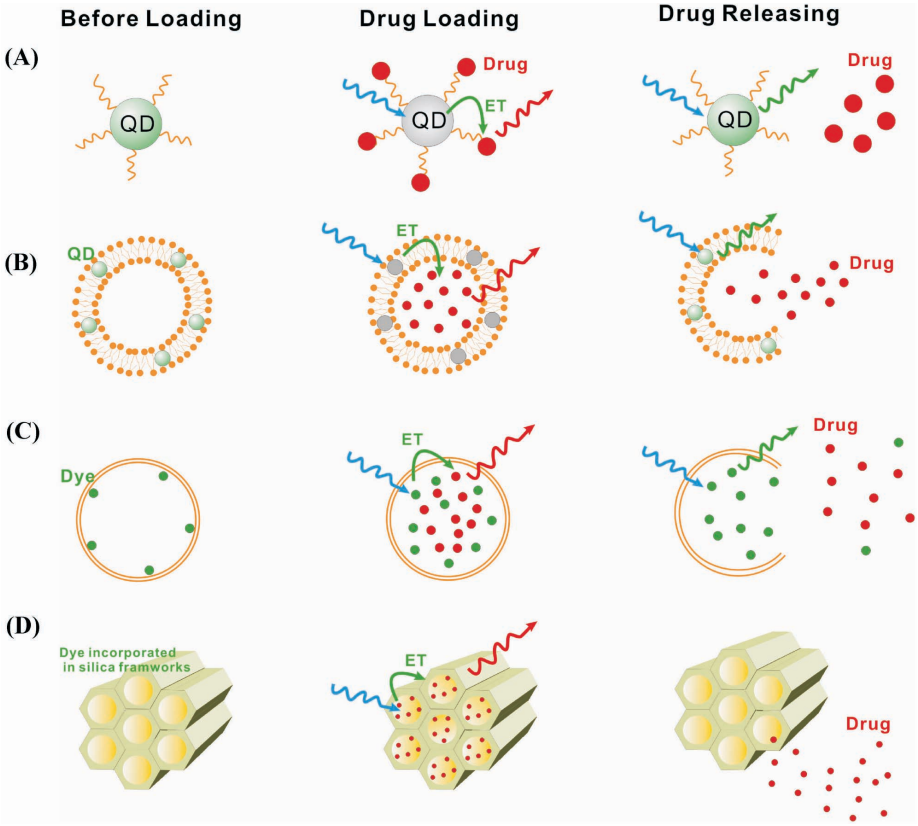

ACKNOWLEDGEMENTS

This study was supported by the Grants MED-099-PP-04 and NM-099-PP-01 from the National Health Research Institutes of Taiwan and grants NSC 95-2120-M-260-002 and NSC 99-2113-M-400-001-MY3, and Biomedical NanoImaging Core Facility of the National Nanoscience and Nanotechnology Program from the National Science Council of Taiwan.

REFERENCES

1. Allen, T. M.; Cullis, P. R. *Science* **2004**, *303*, 1818-1822.
2. Peer, D.; Karp, J. M.; Hong, S.; Farokhzad, O. C.; Margalit, R.; Langer, R. *Nat. Nanotechnol.* **2007**, *2*, 751-760.
3. Moghimi, S. M.; Hunter, A. C.; Murray, J. C. *FASEB J.* **2005**, *19*, 311-330.
4. Wagner, E. *Expert. Opin. Biol. Ther.* **2007**, *7*, 587-593.
5. Sergeeva, A.; Kolonin, M. G.; Molldrem, J. J.; Pasqualini, R.; Arap, W. *Adv. Drug Deliv. Rev.* **2006**, *58*, 1622-1654.
6. Ganta, S.; Devalapally, H.; Shahiwala, A.; Amiji, M. *J. Control Release* **2008**, *126*, 187-204.
7. Shim, W. S.; Kim, J. H.; Kim, K.; Kim, Y. S.; Park, R. W.; Kim, I. S.; Kwon, I. C.; Lee, D. S. *Int. J. Pharm.* **2007**, *331*, 11-18.
8. Bae, Y.; Nishiyama, N.; Fukushima, S.; Koyama, H.; Yasuhiro, M.; Kataoka, K. *Bioconjug. Chem.* **2005**, *16*, 122-130.
9. Lai, P. S.; Lou, P. J.; Peng, C. L.; Pai, C. L.; Yen, W. N.; Huang, M. Y.; Young, T. H.; Shieh, M. J. *J. Controlled Release* **2007**, *122*, 39-46.
10. Na, K.; Lee, K. H.; Lee, D. H.; Bae, Y. H. *Eur. J. Pharm. Sci.* **2006**, *27*, 115-122.
11. Hayashi, H.; Kono, K.; Takagishi, T. *Biochim. Biophys. Acta* **1996**, *1280*, 127-134.
12. Cavallaro, G.; Campisi, M.; Licciardi, M.; Ogris, M.; Giammona, G. *J. Controlled Release* **2006**, *115*, 322-334.
13. Torchilin, V. *Eur. J. Pharm. Biopharm.* **2009**, *71*, 431-444.
14. Motornov, M.; Roiter, Y.; Tokarev, I.; Minko, S. *Prog. Polym. Sci.* **2010**, *35*, 174-211.
15. Medintz, I. L.; Mattoussi, H. *Phys. Chem. Chem. Phys.* **2009**, *11*, 17-45.
16. Algar, W. R.; Krull, U. J. *Anal. Bioanal. Chem.* **2008**, *391*, 1609-1618.
17. Xu, H. X.; Sha, M. Y.; Wong, E. Y.; Uphoff, J.; Xu, Y. H.; Treadway, J. A.; Truong, A.; O'Brien, E.; Asquith, S.; Stubbins, M.; Spurr, N. K.; Lai, E. H.; Mahoney, W. *Nucleic Acids Res.* **2003**, *31*, e43.
18. Ho, Y. P.; Kung, M. C.; Yang S.; Wang, T. H. *Nano Lett.*

2005, *5*, 1693-1697.
19. Choi, H. S.; Frangioni, J. V. *Mol Imaging.* **2010**, *9*, 291-310.
20. Rosenholm, J. M.; Sahlgren, C.; Lindén, M. *Nanoscale* **2010**, *2*, 1870-1883.
21. Shubayev, V. I.; Pisanic, Jr., T. R.; Jin, S. *Adv. Drug Delivery Rev.* **2009**, *61*, 467-477.
22. Wang, M.; Thanou, M. *Pharmacol. Res.* **2010**, *62*, 90-99.
23. Rapoport, N. *Prog. Polym. Sci.* **2007**, *32*, 962-990.
24. Ulbrich, K.; Etrych, T.; Chytil, P.; Jelinkova, M.; Rihova, B. *J. Drug Target* **2004**, *12*, 477-489.
25. Schafer, F. Q.; Buettner, G. R. *Free Radical Biol. Med.* **2001**, *30*, 1191-1212.
26. Park, C.; Kim, H.; Kim, S.; Kim, C. *J. Am. Chem. Soc.* **2009**, *131*, 16614-16615.
27. Squire, A.; Bastiaens, P. I. H. *J. Microsc.* **1999**, *193*, 36-49.
28. Lakowicz, J. R.; Berndt, K. *Rev. Sci. Instrum.* **1991**, *62*, 1727-1734.
29. Gadella, T. W. J. J.; Jovin, T. M.; Clegg, R. M. *Biophys. Chem.* **1993**, *48*, 221-239.
30. Verveer, P. J.; Squire, A.; Bastiaens, P. I. H. *Biophys. J.* **2000**, *78*, 2127-2137.
31. Medintz, I. L.; Uyeda, H. T.; Goldman, E. R.; Mattoussi, H. *Nat. Mater.* **2005**, *4*, 435-446.
32. Zhang, C. Y.; Yeh, H. C.; Kuroki, M. T.; Wang, T. H. *Nat. Mater.* **2005**, *4*, 826-831.
33. Ho, Y. P.; Chen, H. H.; Leong K. W.; Wang, T. H. *J. Controlled Release* **2006**, *116*, 83-89.
34. Chen, H. H.; Ho, Y. P.; Jiang, X.; Mao, H. Q.; Wang T. H.; Leong, K. W. *Mol. Ther.* **2008**, *16*, 324-332.
35. Chen, H. H.; Ho, Y. P.; Jiang, X.; Mao, H. Q.; Wang T. H.; Leong, K. W. *Nano Today* **2009**, *4*, 125-134.
36. Chi, C. W.; Lao, Y. H.; Li, Y. S.; Chen, L. C. *Biosens. Bioelectron.* **2011**, *26*, 3346-3352.
37. Chen, A. A.; Derfus, A. M.; Khetani, S. R.; Bhatia, S. N. *Nucleic Acids Res.* **2005**, *33*, e190.
38. Tan, W. B.; Jiang, S.; Zhang, Y. *Biomaterials* **2007**, *28*, 1565-1571.
39. Qi, L.; Gao, X. *ACS Nano* **2008**, *2*, 1403-1410.
40. Lee, H.; Kim, I.-K.; Park, T. G. *Bioconjugate Chem.* **2010**, *21*, 289-295.
41. Bagalkot, V.; Zhang, L.; Levy-Nissenbaum, E.; Jon, S.; Kantoff, P. W ; Langer R.; Farokhzad, O. C. *Nano Lett.* **2007**, *7*, 3065-3070.
42. Gopalakrishnan, G.; Danelon, C.; Izewska, P.; Prummer, M.; Bolinger, P. Y.; Geissb€uhler, I.; Demurtas, D.; Dubochet J.; Vogel, H. *Angew. Chem., Int. Ed.* **2006**, *45*, 5478-5483.
43. Al-Jamal, W. T.; Al-Jamal, K. T.; Bomans, P. H.; Frederik, P. M.; Kostarelos, K. *Small* **2008**, *4*, 1406-1415.
44. Al-Jamal, W. T.; Al-Jamal, K. T.; Tian, B.; Cakebread, A.; Halket, J. M.; Kostarelos, K. *Mol. Pharm.* **2009**, *6*, 520-530.
45. Weng, K. C.; Noble, C. O.; Papahadjopoulos-Sternberg, B.; Chen, F. F.; Drummond, D. C.; Kirpotin, D. B.; Wang, D.; Hom, Y. K.; Hann B.; Park, J. W. *Nano Lett.* **2008**, *8*, 2851-2857.
46. Tian, B.; Al-Jamal, W. T.; Al-Jamal, K. T.; Kostarelos, K. *Int. J. Pharm.* **2011**, *416*, 443-447.
47. Suzuki, M.; Husimi, Y.; Komatsu, H.; Suzuki, K.; Douglas, K. T. *J. Am. Chem. Soc.* **2008**, *130*, 5720-5725.
48. Chen, H.; Kim, S.; Li, L.; Wang, S.; Park, K.; Cheng, J. X. *Proc. Natl. Acad. Sci. U S A*. **2008**, *105*, 6596-6601.
49. Chen, K. J.; Chiu, Y. L.; Chen, Y. M.; Ho, Y. C.; Sung, H. W. *Biomaterials* **2011**, *32*, 2586-2592.
50. Banerjee, S. S.; Chen, D. H. *Nanotechnology* **2008**, *19*, 505104.
51. Lee, C. H; Cheng, S. H.; Huang, I. P.; Souris, J. S.; Yang, C. S.; Mou, C. Y.; Lo, L. W. *Angew Chem. Int. Ed. Engl.* **2010**, *49*, 8214-8219.
52. Single-photon, time-domain FLIM experiments were performed using an inverted microscope (Olympus IX71, Tokyo, Japan) and 470 nm diode laser excitation (Picoquant GmbH, Berlin, Germany), with pulse durations of 50 picoseconds at a repetition rate of 20 MHz. Coherent light from the laser diode was first passed though a polarization-maintaining, single-mode optical fiber, to provide a Gaussian beam profile. The shaped beam was then reflected by a dichroic mirror (F53-470, AHF Analysentechnik AG) and scanning galvanometer (Olympus FV300, Tokyo, Japan) prior to its introduction to the inverted microscope. A 60x water immersion objective of numerical aperture (NA) 1.2 (Olympus, Tokyo, Japan) was used to both deliver the excitation beam and collect fluorescence emission, while a 100 μm diameter confocal pinhole was used to reject out of focus fluorescence. A longpass filter (HQ500LP, Chroma Technology) and bandpass filter (FF01-550/88, Semrock) were used to exclude excitation light from admission to the detector, a high-speed avalanche photodiode (APD) (Micro Photon Devices, Bolzano, Italy). The APD's TTL output and laser diode trigger were passed through a time-correlated, single photon counting (TCSPC) device (PicoHarp300, Picoquant GmbH, Berlin, Germany), with subsequent image processing performed with Symphotime software 5.0 (Picoquant GmbH, Berlin, Germany).
53. HeLa cells were cultured in a humidified, 37 °C atmosphere comprised of 5% CO2 and 95% room air. Cell culture medium, Minimum Essential Medium (MEM; Gibco), was supplemented with 10% fetal bovine serum (FBS; Hyclone). For fluorescence lifetime measurements cells were plated 24 hours before each experiment, then given 5 μg/mL doxorubicin or 50 ug/mL MSN-dox for 24 hours.